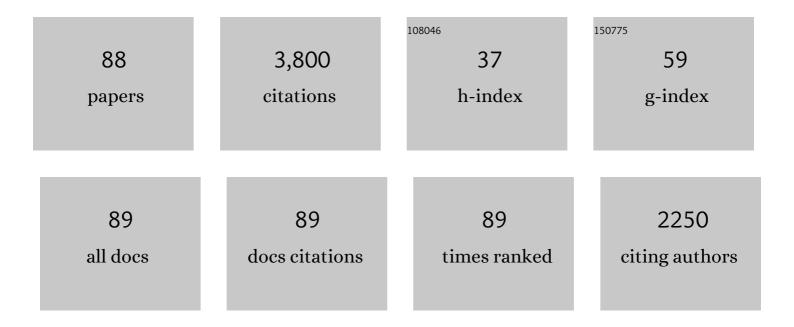
## Mingzhong Zhang

List of Publications by Year in descending order

Source: https://exaly.com/author-pdf/6852820/publications.pdf

Version: 2024-02-01



#	Article	IF	CITATIONS
1	Dynamic compressive behaviour of recycled tyre steel fibre reinforced concrete. Construction and Building Materials, 2022, 316, 125896.	3.2	41
2	Experimental and analytical study of bond between basalt FRP bars and geopolymer concrete. Construction and Building Materials, 2022, 315, 125461.	3.2	21
3	Lattice Boltzmann modelling of ionic diffusivity in non-saturated limestone blended cement paste. Construction and Building Materials, 2022, 316, 126060.	3.2	6
4	Pervious concrete with secondarily recycled low-quality brick-concrete demolition residue: Engineering performances, multi-scale/phase structure and sustainability. Journal of Cleaner Production, 2022, 341, 130929.	4.6	22
5	Pore structure of geopolymer materials and its correlations to engineering properties: A review. Construction and Building Materials, 2022, 328, 127064.	3.2	45
6	3D printing geopolymers: A review. Cement and Concrete Composites, 2022, 128, 104455.	4.6	48
7	Experimental study on static and dynamic properties of fly ash-slag based strain hardening geopolymer composites. Cement and Concrete Composites, 2022, 129, 104481.	4.6	31
8	Total recycling of low-quality urban-fringe construction and demolition waste towards the development of sustainable cement-free pervious concrete: The proof of concept. Journal of Cleaner Production, 2022, 352, 131464.	4.6	17
9	Multiscale modelling of ionic diffusivity in unsaturated concrete accounting for its hierarchical microstructure. Cement and Concrete Research, 2022, 156, 106766.	4.6	16
10	Effect of recycled polymer fibre on dynamic compressive behaviour of engineered geopolymer composites. Ceramics International, 2022, 48, 23713-23730.	2.3	18
11	Recycling utilization of phosphogypsum in eco excess-sulphate cement: Synergistic effects of metakaolin and slag additives on hydration, strength and microstructure. Journal of Cleaner Production, 2022, 358, 131901.	4.6	33
12	3D meso-scale modelling of tensile and compressive fracture behaviour of steel fibre reinforced concrete. Composite Structures, 2022, 291, 115690.	3.1	22
13	Water absorption behaviour of concrete: Novel experimental findings and model characterization. Journal of Building Engineering, 2022, 53, 104602.	1.6	13
14	Mitigating the damage of ultra-high performance concrete at elevated temperatures using synergistic flame-retardant polymer fibres. Cement and Concrete Research, 2022, 158, 106835.	4.6	19
15	Behaviour of strain hardening geopolymer composites at elevated temperatures. Cement and Concrete Composites, 2022, 132, 104634.	4.6	17
16	Relationship between microstructure and strain-hardening behaviour of 3D printed engineered cementitious composites. Cement and Concrete Composites, 2022, 133, 104677.	4.6	19
17	Engineering properties and sustainability assessment of recycled fibre reinforced rubberised cementitious composite. Journal of Cleaner Production, 2021, 278, 123996.	4.6	44
18	Shear behaviour of inorganic polymer concrete beams reinforced with basalt FRP bars and stirrups. Composite Structures, 2021, 255, 112901.	3.1	22

Mingzhong Zhang

#	Article	IF	CITATIONS
19	Meso-scale modelling of compressive fracture in concrete with irregularly shaped aggregates. Cement and Concrete Research, 2021, 140, 106317.	4.6	98
20	Effect of sand content on engineering properties of fly ash-slag based strain hardening geopolymer composites. Journal of Building Engineering, 2021, 34, 101951.	1.6	17
21	Meso-scale modelling of static and dynamic tensile fracture of concrete accounting for real-shape aggregates. Cement and Concrete Composites, 2021, 116, 103889.	4.6	51
22	Micromechanical analysis of interfacial transition zone in alkali-activated fly ash-slag concrete. Cement and Concrete Composites, 2021, 119, 103990.	4.6	36
23	Experimental and numerical investigation on in-plane impact behaviour of chiral auxetic structure. Composite Structures, 2021, 267, 113922.	3.1	34
24	Fractal analysis of 2D and 3D mesocracks in recycled aggregate concrete using X-ray computed tomography images. Journal of Cleaner Production, 2021, 304, 127083.	4.6	16
25	Two-scale modelling of fracture of magnesium phosphate cement under bending using X-ray computed tomography characterisation. Cement and Concrete Composites, 2021, 121, 104099.	4.6	5
26	Effect of curing temperature on hydration, microstructure and ionic diffusivity of fly ash blended cement paste: A modelling study. Construction and Building Materials, 2021, 297, 123834.	3.2	22
27	Effect of recycled tyre polymer fibre on engineering properties of sustainable strain hardening geopolymer composites. Cement and Concrete Composites, 2021, 122, 104167.	4.6	58
28	Rheological behaviour of low-heat Portland cement paste with MgO-based expansive agent and shrinkage reducing admixture. Construction and Building Materials, 2021, 304, 124583.	3.2	18
29	In-situ X-ray tomographic imaging of microstructure evolution of fly ash and slag particles in alkali-activated fly ash-slag paste. Composites Part B: Engineering, 2021, 224, 109221.	5.9	23
30	Behaviour of recycled tyre polymer fibre reinforced concrete at elevated temperatures. Cement and Concrete Composites, 2021, 124, 104257.	4.6	28
31	Experimental study on flexural behaviour of prefabricated concrete beams with double-grouted sleeves. Engineering Structures, 2021, 248, 113237.	2.6	10
32	Three-Dimensional Modeling of Transport Properties in Hardened Cement Paste Using Metal Centrifugation-Based Pore Network. Journal of Materials in Civil Engineering, 2021, 33, .	1.3	6
33	Flexural fatigue behaviour of recycled tyre polymer fibre reinforced concrete. Cement and Concrete Composites, 2020, 105, 103441.	4.6	52
34	Fiber-reinforced geopolymer composites: A review. Cement and Concrete Composites, 2020, 107, 103498.	4.6	337
35	The evolution of interfacial transition zone in alkali-activated fly ash-slag concrete. Cement and Concrete Research, 2020, 129, 105963.	4.6	76
36	Engineering properties of strain hardening geopolymer composites with hybrid polyvinyl alcohol and recycled steel fibres. Construction and Building Materials, 2020, 261, 120585.	3.2	40

MINGZHONG ZHANG

#	Article	IF	CITATIONS
37	Behaviour of recycled tyre polymer fibre reinforced concrete under dynamic splitting tension. Cement and Concrete Composites, 2020, 114, 103764.	4.6	38
38	A new understanding of the effect of filler minerals on the precipitation of synthetic C–S–H. Journal of Materials Science, 2020, 55, 16455-16469.	1.7	6
39	Multiscale micromechanical analysis of alkali-activated fly ash-slag paste. Cement and Concrete Research, 2020, 135, 106141.	4.6	109
40	Modelling of 3D microstructure and effective diffusivity of fly ash blended cement paste. Cement and Concrete Composites, 2020, 110, 103586.	4.6	31
41	Experimental study on engineering properties of concrete reinforced with hybrid recycled tyre steel and polypropylene fibres. Journal of Cleaner Production, 2020, 259, 120914.	4.6	81
42	Relationships between microstructure and transport properties in mortar containing recycled ceramic powder. Journal of Cleaner Production, 2020, 263, 121384.	4.6	34
43	Efficiency of electrochemical extraction of chlorides in fly ash concrete using carbon fibre mesh anode. Construction and Building Materials, 2020, 249, 118717.	3.2	13
44	A novel framework for modelling the 3D mesostructure of steel fibre reinforced concrete. Computers and Structures, 2020, 234, 106251.	2.4	27
45	Engineering properties of crumb rubber alkali-activated mortar reinforced with recycled steel fibres. Journal of Cleaner Production, 2019, 238, 117950.	4.6	61
46	Three-dimensional virtual microstructure generation of porous polycrystalline ceramics. Ceramics International, 2019, 45, 21647-21656.	2.3	7
47	Experimental study on a precast beam-column joint with double grouted splice sleeves. Engineering Structures, 2019, 199, 109589.	2.6	52
48	An integrated framework for modelling virtual 3D irregulate particulate mesostructure. Powder Technology, 2019, 355, 808-819.	2.1	24
49	Mechanical behaviour of grouted sleeve splice under uniaxial tensile loading. Engineering Structures, 2019, 186, 421-435.	2.6	69
50	Experimental study on dynamic compressive behaviour of recycled tyre polymer fibre reinforced concrete. Cement and Concrete Composites, 2019, 98, 95-112.	4.6	56
51	Internal curing of alkali-activated fly ash-slag pastes using superabsorbent polymer. Cement and Concrete Research, 2019, 116, 179-190.	4.6	95
52	Influence of moisture condition on chloride diffusion in partially saturated ordinary Portland cement mortar. Materials and Structures/Materiaux Et Constructions, 2018, 51, 1.	1.3	43
53	Modelling of irregular-shaped cement particles and microstructural development of Portland cement. Construction and Building Materials, 2018, 168, 362-378.	3.2	37
54	Workability and mechanical properties of alkali-activated fly ash-slag concrete cured at ambient temperature. Construction and Building Materials, 2018, 172, 476-487.	3.2	305

MINGZHONG ZHANG

#	Article	IF	CITATIONS
55	Mechanisms of autogenous shrinkage of alkali-activated fly ash-slag pastes cured at ambient temperature within 24â€ <sup>-</sup> h. Construction and Building Materials, 2018, 171, 377-387.	3.2	89
56	Numerical simulation of the effect of cement particle shapes on capillary pore structures in hardened cement pastes. Construction and Building Materials, 2018, 173, 615-628.	3.2	48
57	Pore-scale modelling of relative permeability of cementitious materials using X-ray computed microtomography images. Cement and Concrete Research, 2017, 95, 18-29.	4.6	68
58	Mechanical and thermal properties of graphene sulfonate nanosheet reinforced sacrificial concrete at elevated temperatures. Construction and Building Materials, 2017, 153, 682-694.	3.2	33
59	Effects of graphene sulfonate nanosheets on mechanical and thermal properties of sacrificial concrete during high temperature exposure. Cement and Concrete Composites, 2017, 82, 252-264.	4.6	60
60	Numerical modeling of drying shrinkage deformation of cement-based composites by coupling multiscale structure model with 3D lattice analyses. Computers and Structures, 2017, 178, 88-104.	2.4	43
61	Mechanical Properties and Damage Evolution of Siliceous Concrete Subjected to Elevated Temperatures. Key Engineering Materials, 2016, 711, 488-495.	0.4	1
62	Experimental study on flexural behaviour of inorganic polymer concrete beams reinforced with basalt rebar. Composites Part B: Engineering, 2016, 93, 174-183.	5.9	47
63	Mechanical and physicochemical properties of ferro-siliceous concrete subjected to elevated temperatures. Construction and Building Materials, 2016, 122, 743-752.	3.2	33
64	Behaviour of inorganic polymer concrete columns reinforced with basalt FRP bars under eccentric compression: An experimental study. Composites Part B: Engineering, 2016, 104, 44-56.	5.9	59
65	Computational technology for analysis of 3D meso-structure effects on damage and failure of concrete. International Journal of Solids and Structures, 2016, 80, 310-333.	1.3	168
66	Micromechanical modelling of deformation and fracture of hydrating cement paste using X-ray computed tomography characterisation. Composites Part B: Engineering, 2016, 88, 64-72.	5.9	63
67	Thermal behavior of siliceous and ferro-siliceous sacrificial concrete subjected to elevated temperatures. Materials and Design, 2016, 95, 470-480.	3.3	25
68	Discrete Lattice Model of Quasi-Brittle Fracture in Porous Graphite. Materials Performance and Characterization, 2014, 3, 414-428.	0.2	4
69	A Lattice-spring Model for Damage Evolution in Cement Paste. , 2014, 3, 1854-1859.		4
70	Microstructure-informed modelling of damage evolution in cement paste. Construction and Building Materials, 2014, 66, 731-742.	3.2	48
71	Multiscale lattice Boltzmann-finite element modelling of chloride diffusivity in cementitious materials. Part II: Simulation results and validation. Mechanics Research Communications, 2014, 58, 64-72.	1.0	33
72	Fracture Energy of Graphite from Microstructure-informed Lattice Model. , 2014, 3, 1848-1853.		7

5

MINGZHONG ZHANG

#	Article	IF	CITATIONS
73	Site-bond Modelling of Structure-failure Relations in Quasi-brittle Media. , 2014, 3, 1872-1877.		2
74	Transport properties in unsaturated cement-based materials – A review. Construction and Building Materials, 2014, 72, 367-379.	3.2	83
75	Multiscale lattice Boltzmann-finite element modelling of chloride diffusivity in cementitious materials. Part I: Algorithms and implementation. Mechanics Research Communications, 2014, 58, 53-63.	1.0	38
76	Pore-scale modelling of 3D moisture distribution and critical saturation in cementitious materials. Construction and Building Materials, 2014, 64, 222-230.	3.2	26
77	Meso-scale site-bond model for elasticity: theory and calibration. Materials Research Innovations, 2014, 18, S2-982-S2-986.	1.0	7
78	Microstructure-based modeling of permeability of cementitious materials using multiple-relaxation-time lattice Boltzmann method. Computational Materials Science, 2013, 68, 142-151.	1.4	56
79	Modeling of ionic diffusivity in non-saturated cement-based materials using lattice Boltzmann method. Cement and Concrete Research, 2012, 42, 1524-1533.	4.6	71
80	Computational investigation on mass diffusivity in Portland cement paste based on X-ray computed microtomography (μCT) image. Construction and Building Materials, 2012, 27, 472-481.	3.2	123
81	Microstructure-based modeling of water diffusivity in cement paste. Construction and Building Materials, 2011, 25, 2046-2052.	3.2	40
82	Modelling of time dependency of chloride diffusion coefficient in cement paste. Journal Wuhan University of Technology, Materials Science Edition, 2010, 25, 687-691.	0.4	8
83	Un método numérico-estadÃstico para determinar el volumen elemental representativo (VER) de la pasta de cemento en la medición de la difusividad. Materiales De Construccion, 2010, 60, 7-20.	0.2	32
84	Shrinkage Performance and Cracking Resistance Mechanism of Rubberized Lightweight Aggregate Concrete with Polymer. Key Engineering Materials, 2008, 385-387, 817-820.	0.4	1
85	Pore Properties of Eco-Material for Erosion Control of Slope and its Fractal Features. Key Engineering Materials, 2008, 385-387, 461-464.	0.4	Ο
86	Flexural fatigue behavior of layered hybrid fiber reinforced concrete. Journal Wuhan University of Technology, Materials Science Edition, 2007, 22, 560-563.	0.4	8
87	Experimental Study on the Flexural Fatigue Damage Evolution of Layered Fiber Reinforced Concrete. Key Engineering Materials, 0, 385-387, 673-676.	0.4	1
88	Nonlinear Stability Analysis on the Concrete Casting Step of Long-Span Concrete-Filled Steel Tube Arch Bridge. Materials Science Forum, 0, 614, 275-282.	0.3	0